Biochimica et Biophysica Acta, 551 (1979) 432—447

BBA 78298

TRANSPORT CHARACTERISTICS OF FROG GASTRIC MEMBRANES

E. RABON , G. SACCOMANI, D.K. KASBEKAR * and G. SACHS **

Laboratory of Membrane Biology, University Station, University of Alabama in Birmingham, Birmingham, AL 35294 (U.S.A.)

(Received July 4th, 1978)

Key words: Transport properties; Proton pump; Cl^- pump; (Frog gastric membrane)

Summary

ATP-induced transport by fractions of frog gastric microsomes prepared either by density gradient centrifugation or by free flow electrophoresis were K^+ dependent and hence considered due to a K^+-activated ATPase. Significant activity of this enzyme was, however, only found in the anodic peak of the free flow electrophoretic separation, which in addition to separating transporting from non-transporting particles, also separated membranes containing a phosphorylatable peptide (M_r = 105 000) region as the major peptide on SDS-polyacrylamide gel electrophoresis from those containing a peptide (M_r = 44 000) on SDS-polyacrylamide gel electrophoresis. H^+ uptake, measured either by acridine orange or 3,3'-diethyloxadicarbocyanine + tetrachlorosalicylanilide absorbance changes was dependent on K^+ intravesicularly. Using $^{86}Rb^+$, active extrusion of the cation followed ATP addition. SCN^-, an inhibitor of acid secretion did not affect the latter, but blocked signals due to H^+ uptake, in contrast to mammalian preparations.

Introduction

Frog gastric mucosa is the best studied in vitro model of acid secretion [1—4]. Several conclusions have been drawn from observations of the functioning gastric mucosal sheet and metabolite assays of parietal cell regions. These findings may be summarized as follows: (a) the H^+ pump may be electrogenic [1]; (b) an independent Cl^- pump is present [1,5]; (c) H^+ secretion is abso-

* Present address: Department of Physiology, Georgetown University, Washington, DC
** To whom correspondence should be addressed.
Abbreviations: TCS, tetrachlorosalicylanilide; DOCC, 3,3'-diethyloxacarbodicyanine; $DiBac_4(5)$, bis-[1,3-dibutyl-barbituric acid-(5)]pentamethinoxonol; Pipes, piperazine-*N*,*N*'-bis(2-ethanesulfonic acid).

lutely O_2 dependent and while changes in the redox state of mitochondria preceed the onset of acid secretion these component changes do not indicate an ATP-dependent pump [4,5]; (d) changes in high energy phosphates are not in favor of such a pump [7]; (e) microsomal fractions contain a K^+-activated ATPase [8].

Although analysis of metabolite profiles in the dog [9] also do not provide direct evidence for an ATP-driven H^+ pump, studies of mammalian gastric membranes show the presence of an electroneutral ATP-dependent H^+ for K^+ exchange in membrane vesicles, clearly implicating an ATP-driven H^+ pump [10,11]. This pump is present in dog [12,13] rabbit [14], hog [15,16] and man [17].

Characterization of the frog microsomal system which indicates the existence of K^+-sensitive ATPase, has previously been described [8,14]. Since the K^+-ATPase of gastric mucosa in other species exhibits transport properties, membranes isolated by centrifugal and electrophoretic techniques have been studied. Significant similarities and differences exist between preparations of mammalian and amphibian membranes.

Materials and Methods

Preparation. Following the 3 M NaCl lysis of surface cells [18] the deeper cell layers from the gastric fundic mucosa of seven large bullfrogs (*Rana catesbina*) were removed by scraping with a microscope slide. These scrapings were homogenized with 10 strokes at 2000 rev./min in a teflon-glass homogenizer in cold 0.3 M sucrose, 5 mM Tris-HCl, pH 7.4. Differential centrifugation of this homogenate included spins of 10 min at $800 \times g$, 15 min at $10\,000 \times g$ and 1 h at $100\,000 \times g$.

Free flow electrophoresis. The crude microsomal pellet was resuspended in 0.3 M sucrose, 8 mM acetic acid and 8 mM Tris-HCl, pH 7.4, spun down once for 1 h at $100\,000 \times g$ and resuspended in the same buffer. This suspension was loaded on the FF5 free flow electrophoresis unit developed by Hannig et al. [19] (Biochemical Instruments, NY) and separation was carried out as previously described [16]. The sample which was injected at 1 ml/h was separated into 90 fractions which were collected at 4°C. Electrophoresis was interrupted every 30 min to remove mucous build-up at the curtain entry port. Conditions in the run were: $120 \pm 10\%$ V/cm, 147 mA, temperature 7.4 ± 0.2°C and electrophoresis buffer flow 4 ml/fraction per h. The resolved protein peaks, monitored as 280 nm absorption profiles were pooled, spun down for 1 h at $100\,000 \times g$ and resuspended in 0.3 M sucrose, 2 mM piperazine-*N*,*N*′-bis(2-ethane sulfonic acid) (Pipes)/Tris, pH 7.4.

Density gradient centrifugation. In other experiments, 2 ml of the microsomal fraction was loaded onto step gradients consisting of successive 5-ml steps of 7% Ficoll (w/w) in 0.3 M sucrose, 22% sucrose and 30% sucrose (w/w). Centrifugation was carried out in a Sorvall AH-627 swinnging bucket rotor spun at 25 000 rev./min for 14 h. The bands were removed by Pasteur pipette. Protein was determined by the method of Lowry et al. [20].

Phosphorylation. 20 μg of membrane protein was added at 4°C to 0.5 ml of a mixture containing 150 mM choline chloride, 5 μM ATP containing 0.2 μCi

[γ-^{32}P]ATP, 10 μM $MgCl_2$ and 5 mM Pipes/Tris (pH 7.4) with or without 20 mM KCl. After a 15 s incubation, 0.5 ml of ice-cold 12% trichloroacetic acid containing 0.1 mM P_i and 1.0 mM ATP was added to stop the reaction. The precipitate was then filtered on HAWP (0.45 μm) millipores and washed three times with 3.0 ml of 150 mM choline chloride, 10 μM $MgCl_2$ and 5 mM Pipes/Tris, pH 7.4. Radioactivity was measured by an LKB 81000 liquid scintillation counter. For gel electrophoresis, 20 μg of membrane protein was added at 4°C to 80 μl total volume containing 0.1 μM ATP, 2.0 μCi [γ-^{32}P]ATP, 10 μM $MgCl_2$ and 20 mM Tris/HCl (pH 7.4) with or without 20 mM KCl. Following a 15 s incubation at 4°C, the membranes were solubilized with 80 μl of 2.0% SDS/2.0% β-mercaptoethanol and gel electrophoresis carried out immediately at 4°C.

Polyacrylamide gel electrophoresis. Gel electrophoresis was performed as previously described [13]. Briefly, in this procedure 20 μg of solubilized membrane protein (80 μl) was layered on a a 1.0 cm stacking gel system consisting of 3.5% polyacrylamide, pH 6.8, layered on top of 10% polyacrylamide, pH 8.6. A current of 1 mA/gel was applied for 1 h to run the sample through the stacking gel. Afterwards, the current was increased to 2.5 mA/gel, until the completion of the gel run. At this point, the ^{32}P-labelled gels were sliced into 1.5-mm sections and incubated in 200 μl of 50% H_2O_2 overnight at 60°C. In the morning the samples were cooled, diluted in 10 ml of Aquasol and counted in the LKB 81000 liquid scintillation counter. The gels to be stained with Coomassie blue were washed overnight in a solution of 7.5% acetic acid and 30% methanol and then stained with 0.25% Coomassie blue in 7.5% acetic acid/30% methanol for 6 h. After 48 h of destaining, the gels were scanned at 550 nm in a Gilford 2400 Spectrophotometer equipped with a gel scanner at 1.0 cm/min scan rate using a slit width of 0.05 mm.

ATPase assay. ATPase activity was assayed in 1 ml of medium containing 10 μg membrane protein, 40 mM Tris-HCl, pH 7.4, 2 mM $MgCl_2$ and 2 mM ATP (disodium salt). Optional additions to the assay included 20 mM KCl, 20 mM Na^+ or $KHCO_3$, 20 mM NaSCN and 10 μg of oligomycin. NaSCN and oligomycin were incubated with the membrane protein for 10 min at room temperature before the start of the assay. After incubation at 37°C for 15 min, the inorganic phosphate released was measured either by the method of Yoda and Hokin [21]or Fiske-Subarrow [22]. The term 'basal ATPase' refers to the activity observed when the only activating ion present was Mg^{2+}.

Dithionite-reduced spectrum. 0.5 mM sodium dithionite ($Na_2S_2O_4$) was added to a 350 μl sample in a microcuvette containing 1 mg/ml membrane protein suspended in 20 mM Tris-HCl, pH 7.4. After manually deriving a baseline for reference and sample cuvettes, solid $Na_2S_2O_4$ was added to the sample cuvette to a final concentration of 0.5 mM. The absorption difference between this and an untreated reference membrane sample was scanned from 400 to 650 nm in the Aminco DW-2 split-beam spectrophotometer. Wavelength pairs and extinction coefficients used in the calculation of pigment concentration were those published by Chance and Williams [23].

Transport activity. Proton gradient formation was assessed by measurement of the absorbance change of 5 μM acridine orange and potential difference was assessed by the absorbance changes of 4 μM 3,3′-diethyloxadicarbocyanine

iodide (DOCC) or the oxonol dye bis-[1,3-dibutyl-barbituric acid-(5)]pentamethinoxonol (diBAC$_4$(5)) following ATP addition. The addition of a protonophore in the presence of DOCC and ATP induced H^+ diffusion potential resulting in dye absorbance changes quantitatively related to the H^+ gradient. As previously described [24], the membrane material was suspended in 150 mM KCl, 2 mM $MgCl_2$ and 2 mM Pipes/Tris (pH 7.4) to 0.3 mg/ml final concentration. For chloride-free experiments, K_2SO_4 and $MgSO_4$ were substituted for KCl and $MgCl_2$, respectively. After 2 h room temperature preincubation, either 5 μM acridine orange, 4 μM DOCC ± 6 μM tetrachlorsalicylanilide (TCS) or 4 μM diBAC$_4$(5) was added to 350 μl of the suspension. Either $MgCl_2$/ATP (pH 7.4) or $MgSO_4$/ATP (pH 7.4) (0.6 mM final concentration) was added and absorbance changes monitored at the appropriate wavelength pairs (i.e. acridine orange, 496 to 446 nm; DOCC, 588—636 nm; diBAC$_4$(5), 600—640 nm).

$^{86}Rb^+$ efflux. The membrane fractions were suspended in a solution consisting of 75 mM RbCl, 2 mM $MgCl_2$, 2 mM Pipes/Tris, pH 6.1, 6.6 μCi $^{86}Rb^+$ at a final protein concentration of 1 mg/ml. In some experiments 75 mM KCl was used. After a 2 h room temperature preincubation, total uptake of $^{86}Rb^+$ was measured by placing duplicate 20-μl aliquots in a stop solution consisting of 500 μl of ice-cold 75 mM choline chloride, 2 mM $MgSO_4$, 0.135 M sucrose and 2 mM Pipes/Tris, pH 6.1. This suspension was filtered on HAWP millipore filters (0.45 μm) and washed four times with 2.5 ml ice-cold stop solution. Following the addition of 2 mM MgATP, pH 6.1, further 20-μl aliquots were removed and filtered as above at different times. For some experiments, a 10 min 23°C incubation with 20 mM NaSCN preceded the addition of ATP. After drying, the filters were placed in 10 ml of Amersham ACS counting fluid and counted on an LKB 81000 liquid scintillation counter.

Materials. 3,3'-Diethyloxadicarbocyanine (DOCC) iodide was purchased from Eastman. diBAC$_4$(5) was a gift from Dr. A. Waggoner, acridine orange was a gift from Dr. J. Mentor. ^{86}RbCl was purchased from New England Nuclear. Bullfrogs were purchased by Animal Services from Jaques Wiel Co. Chemicals used in biochemical assays were obtained from Sigma. All chemicals were of reagent grade.

Results

Resolution of microsomal membranes

Free flow electrophoresis. The amphibian microsomal pellet, prepared as outlined in Materials and Methods, was a heterogeneous material containing what appeared to be both clear and pigmented membranes. Fig. 1 indicates that this material, when washed and resuspended in isotonic, Tris/acetate buffer, pH 7.4, could be resolved by the free flow electrophoresis procedure into two separate protein peaks with some additional material between these peaks. This resolution was characteristic of every amphibian microsomal sample tested. Preparational variations were restricted to changes in the proportions of these two major peaks.

Discontinuous sucrose gradient. Membrane material designated GI (Ficoll-sucrose), GII (20% sucrose) or GIII (29% sucrose) was found at each interface on the step gradient. The lightest band (GI) produced the smallest yield of

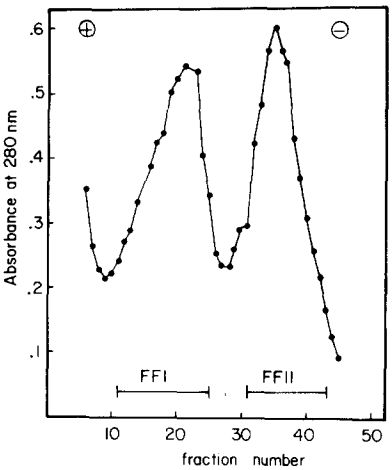

Fig. 1. Electrophoretic resolution of membrane-bound proteins utilizing the Hannig model 5, free flow electrophoresis apparatus. Material from the two major 280 nm absorbance peaks, FFI (tubes 11—25) and FFII (tubes 31—43) was pooled and prepared as detailed in Materials and Methods.

materials. This membrane fraction, trapped on the top of the Ficoll-sucrose interface was cleanly separated from the heavier material. The GII material was trapped at the sucrose-ficoll-22% sucrose interface. Like the GI material, the quantity of this material was low in comparison to the GIII fraction. The 22% sucrose layer contained a diffuse cloud of membrane material concentrating in the 29% sucrose interface. The material at the 29% interface (GIII) was the predominant band on the discontinuous gradient. The 30% sucrose layer also contained a diffuse cloud of material. A pellet was formed at the bottom of the tube.

There appeared to be little color in the ficoll-sucrose band. However, pigmentation progressively increased in the heavier gradient bands. The pellet under the 30% sucrose was heavily pigmented.

Dithionite-reduced spectrum. Fig. 2 shows a dithionite-reduced spectrum for each of the electrophoretically separated fractions (i.e. FFI and FFII). Characteristic absorption peaks identify flavoprotein, cytochromes *b*, $c + c_1$, *a* and a_3. The components identified by those spectra are listed in Table I. This comparison indicated a substantial mitochondrial contamination within the crude microsomal material which was enriched in the second peak. This enrichment in the second fraction was greater for complex IV (i.e. cytochromes *a* and a_3) whose average values increased 3.4-fold over the anodic peak (FFI). For complex III (i.e. cytochromes *b* and c_1) the average increase was 1.8-fold. Absorption peaks characteristic of other microsomal redox systems were not detected in either FFI and FFII.

ATPase activity. Basal Mg^{2+}-ATPase activity was present in every microsomal membrane fraction isolated. The large variations in this activity indicated the presence of a heterogenous population of ATPases. Table II lists this basal Mg^{2+}-ATPase as well as the activity in the presence of the stimulating ions K^+ and HCO_3^- for both free flow and discontinuous sucrose gradient procedures.

Comparison of the basal Mg^{2+}-ATPase activity in the sucrose gradient

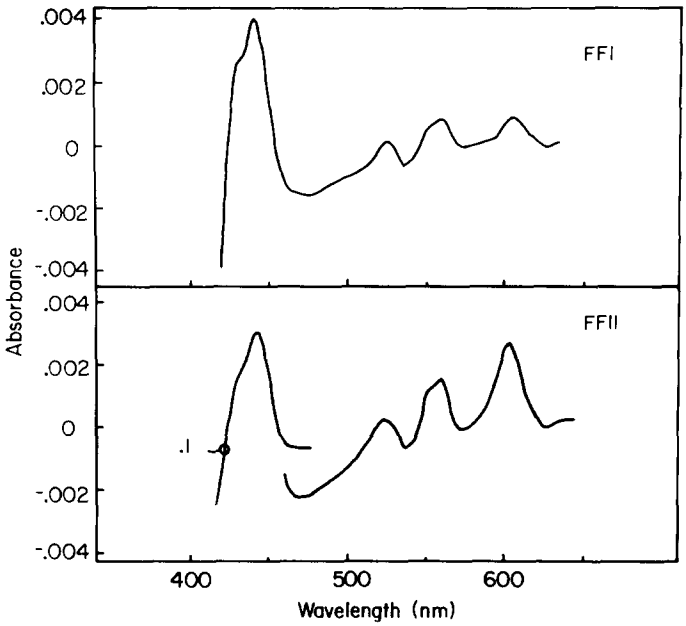

Fig. 2. Comparison of the $Na_2S_2O_4$-reduced spectrum of FFI and FFII. See Materials and Methods for details of procedure. For both FFI and FFII membranes, full scale absorbance on the Aminoc DW-2 split beam system was set at 0.02 absorbance unit. The first bands (shorter wavelengths) in the FFII membrane system were recorded with full scale absorbance sensitivity decreased to 0.1 absorbance unit.

fractions (i.e. GI, GII, GIII) showed that the basal Mg^{2+}-ATPase activity was enriched in the membrane fractions which equilibrated in progressively denser sucrose. Table II shows that the membranes at the 29% sucrose (i.e. GII) interface had an 11-fold increase in activity over the material equilibrated at the sucrose-ficoll interface (i.e. GI). This separation of basal Mg^{2+}-ATPase into fractions with either low or high activity (i.e. GI or GIII) was also achieved by free flow fractionation. At 92.1 $\mu mol \cdot mg^{-1} \cdot h^{-1}$, the Mg^{2+}-ATPase activity of the FII membranes was the highest obtained by either purification procedure.

Enrichment of the HCO_3^--stimulated component of the ATPase activity coincided with that of the basal Mg^{2+}-ATPase. Within the density gradient

TABLE I

IDENTIFICATION OF REDOX COMPONENTS REDUCED BY $Na_2S_2O_4$

Values are given as μmol/mg membrane protein. Wavelength pairs and extinction coefficients used were those determined by Chance and Williams [23].

	Flavo-protein	Cytochrome			
		b	$c + c_1$	*a*	a_3
Microsomal	0.304	0.151	0.132	0.296	0.289
FFI	0.204	0.098	0.074	0.112	0.078
FFII	0.296	0.141	0.158	0.311	0.309

TABLE II

ATPase ACTIVITY IN GRADIENT AND FREE FLOW ELECTROPHORESIS FRACTIONS

Values are expressed as $\mu mol \cdot mg^{-1} \cdot h^{-1}$.

Fraction	Basal Mg^{2+}	Mg^{2+} + 20 mM K^+	ΔK^+	Mg^{2+} + HCO_3^-	ΔHCO_3^-
Microsomal	62.3 ± 6.2 $n = 5$	64.4 ± 7.5 $n = 5$	2.1	100.5 ± 10.3 $n = 3$	38.2
GI	5.2 ± 1.2 $n = 6$	7.0 ± 1.7 $n = 6$	1.8	9.8 ± 2.6 $n = 4$	4.6
GII	42.4 ± 10.8 $n = 4$	39.2 ± 7.1 $n = 4$	—	68.9 ± 14.4 $n = 3$	26.5
GIII	58.2 ± 5.94 $n = 7$	56.6 ± 4.2 $n = 7$	—	83.5 ± 12.8 $n = 4$	25.3
FI	18.0 ± 5.3 $n = 4$	23.7 ± 5.9 $n = 4$	5.8	21.9 ± 20.3 $n = 2$	3.9
FII	92.1 ± 6.2 $n = 5$	96.4 ± 9.5 $n = 3$	4.3	124.9 ± 4.75 $n = 2$	32.8

material this increase in activity was approximately 6-fold from GI to GII. As with the basal Mg^{2+}-ATPase activity, the highest activity obtained was in the free flow fraction, FFII. In the free flow fractions, there was depletion of HCO_3^- stimulation in the FFI fraction with concomitant enrichment in the FFII membranes.

The results of an experiment which assayed the sensitivity of the components of the ATPase reaction to the mitochondrial inhibitor protein are displayed in Table IV. Clearly, most of the activity in the GIII fraction, regardless of the stimulating ion, is sensitive to the mitochondrial inhibitor protein. The GI fraction differs somewhat from the inhibitory pattern observed with the GIII material. In the GI fraction, that component of the ATPase reaction which is stimulated by $KHCO_3$ is partially insensitive to the mitochondrial inhibitor protein. Only 40% of the $KHCO_3$ stimulation is lost by incubation with the mitochondrial inhibitor protein.

K^+-stimulated ATPase activity was highest in the membrane fraction FFI isolated by free flow electrophoresis. In the FFI fraction the K^+-stimulated activity was approximately 6 $\mu mol \cdot mg^{-1} \cdot h^{-1}$. This exceeded that observed in any of the sucrose gradient fractions. In membranes isolated by sucrose gradient fractionation, a slight K^+ stimulation is present in the lightest fraction, but was smaller than that of the FFI. K^+-stimulation does not appear present in the 20% and 29% sucrose fractions, but a small activation could be obscured by the high basal Mg^{2+} activities of these fractions.

The K^+-stimulated ATPase of the FFI fraction was insensitive to both 20 mM NaSCN and oligomycin (2.8 : 1). Table III emphasizes the disparity between Mg^{2+}- and K^+-ATPase sensitivities. The basal Mg^{2+}-ATPase activity was 89% inhibited by oligomycin and 62% by 20 mM NaSCN. This was in contrast to an apparent 16% stimulation of the K^+ component by oligomycin and 36% stimulation by SCN^- of this activity.

Polypeptide pattern. Fig. 3 shows the complex polypeptide pattern of the membrane fractions resolved by free flow electrophoresis. In the microsomal fraction there were two major polypeptide peaks representing 100 000- and

TABLE III

EFFECT OF SCN^- AND OLIGOMYCIN ON BASAL Mg^{2+} AND THE K^+-STIMULATED ATPase ACTIVITY OF THE FFI MEMBRANE FRACTION

Activity expressed as $\mu mol \cdot mg^{-1} \cdot h^{-1}$

	Specific activity			% sensitivity	
	Control	20 mM NaSCN	Oligomycin *	20 mM NaSCN	Oligomycin
Basal Mg^{2+}	21.1 ± 2.7 $n = 4$	8.1 ± 4.2 $n = 2$	2.35 ± 0.8 $n = 3$	−61.6	−88.9
$Mg^{2+} + K^+$	29.4 ± 3.4 $n = 3$	19.4 ± 10.2 $n = 2$	11.9 ± 1.9 $n = 2$	−34.0	−59.5
ΔK^+	8.3	11.3	9.6	+36.1	+15.6

* Oligomycin/protein, 2.8 : 1.

44 000-dalton polypeptides. In addition to these major peaks, four bands accounting for 30% of the total stained protein and five bands accounting for 25% were located between the 100 000 and 44 000 molecular weight region and below the 44 000 molecular weight region, respectively. The first anodic peak (FFI) was enriched both in the 100 000 molecular weight region and in the region between 44 000 and 100 000. In this fraction the 100 000 molecular weight region accounted for approximately 53% of total stained protein. Together with the peptides of molecular weight range 44 000 and 100 000, they accounted for approximately 86% of the Coomassie blue-stained protein in this fraction. The major protein peak of the FFII fraction, the 44 000 molecular weight peak, was 35% of the protein in the FFII membrane fraction. Gradient fractionation showed only poor resolution of those peptides.

Membrane phosphorylation. Incubation of the anodic free flow fraction with [γ-^{32}P]ATP, labelled a component of the trichloroacetic acid precipitate of this material. In FFI, 226 pmol/mg of membrane protein were labelled with ^{32}P. As indicated in Table V, this label was partially sensitive to 20 mM KCl. 46% of the ^{32}P-label was lost if the membranes were phosphorylated in the presence of 20 mM KCl. In contrast to the FFI material, there was little phosphorylation in the FFII fraction. Table V indicates formation of a K^+-insensitive component of only 16 pmol/mg.

The 10% polyacrylamide gel peptide pattern of the 1% SDS/1% β-mercapto-

TABLE IV

ATPase SENSITIVITY OF SUCROSE GRADIENT FRACTIONS TO MITOCHONDRIAL INHIBITOR PROTEIN (MIP)

Activity expressed as $\mu mol \cdot mg^{-1} \cdot h^{-1}$.

		Untreated	MIP-treated
Basal Mg^{2+}	GI	0.14	0
	GIII	84.6	0
$Mg^{2+} + KHCO_3$	GI	6.4	3.8
	GIII	138.0	1.7

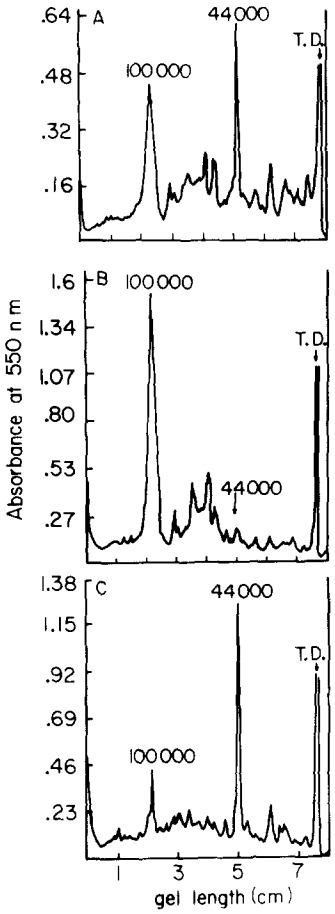

Fig. 3. Polypeptide pattern resulting from 1% SDS/1% β-mercaptoethanol solubilization of the crude microsomal, FFI and FFII membrane systems. See Materials and Methods for details. Molecular weight determinations were calculated by relative mobility in comparison to a series of standards of known molecular weight. (A) Represents the crude microsomal material; (B) the FFI membrane fraction and (C) the FFII membrane fraction (T.D. = tracking dye).

ethanol-solubilized phosphorylated FFI system is presented in Fig. 4. Two areas of the gel were heavily labelled. The first was the 100 000 molecular weight peptide region. From the counts recorded in Fig. 4 in this region 57% of this phosphoprotein was sensitive to 20 mM KCl. The second region was at the end of the gel and did not correspond to an area of peptide stain. These counts are due to free inorganic ^{32}P and low molecular weight glycolipids which are labelled at alkaline pH [13,25].

Transport experiments

Acridine orange. Absorbance signals consistent with the generation of a proton gradient are dependent on previous incubation of the anodic material (FFI) with KCl. The KCl requirement can be fulfilled by prolonged incubations at 4°C, 2 h room temperature incubations or the addition of valinomycin to non-equilibrated material. Under these conditions, ATP addition to the vesicles

TABLE V

[γ-^{32}P]ATP PHOSPHORYLATION OF MEMBRANE FRACTIONS SEPARATED BY FREE FLOW ELECTROPHORESIS

^{32}P-labelled protein is expressed as pmol Pi/mg membrane protein.

^{32}P-labelled protein	Mg^{2+} only	Mg^{2+} + 20 mM K^+	% K^+ sensitive
FFI	266	144	46
FFII	16	19	—

in the presence of 5 μM acridine orange resulted in the absorption changes shown in Fig. 5. This nigericin and tributyltin-sensitive signal (latter results not shown) exhibited an 80 s t_{max} followed by a slow decay to baseline. 10 min equilibration with SCN^- reduced the magnitude of the absorbance change by 86%. The same equilibration procedure with 10 μg of oligomycin (10 μg oligomycin/105 μg protein) reduced the acridine orange signal by 47%. In the presence of oligomycin, the t_{max} was shifted to 140 s. Acridine orange changes were not observed in FFII.

The development of an acridine orange response to the ATP-dependent

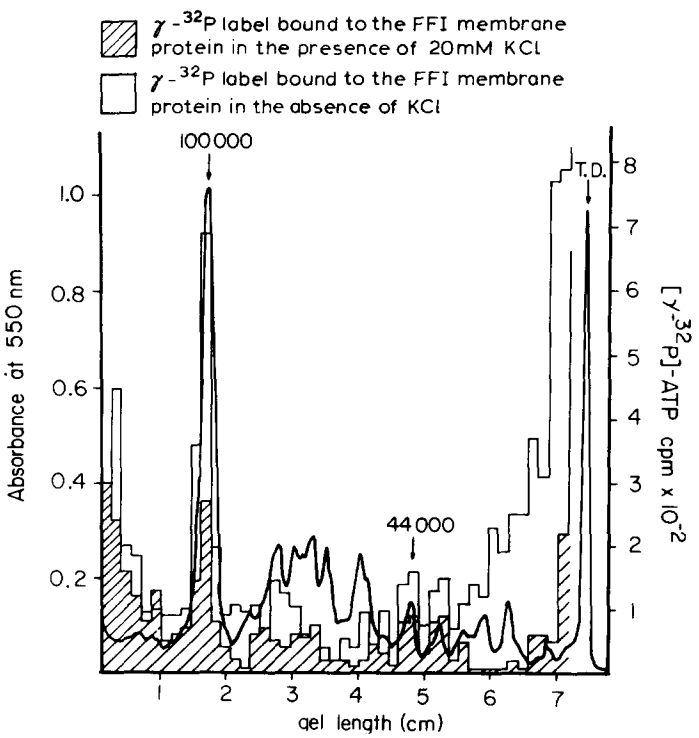

Fig. 4. [γ-^{32}P]ATP phosphorylation pattern of the FFI membrane system. 40 μg of FFI protein was added at 4°C to an 80 μl total volume containing 0.1 μM ATP, 2.0 μCi [γ-^{32}P]ATP, 10 mM $MgCl_2$ and 20 mM Tris-HCl, pH 7.4, with or without 20 mM KCl. After a 15 s incubation at 4°C, the membranes were solubilized in 1.0% SDS/1% β-mercaptoethanol and this material applied to the gel system detailed in Materials and Methods. Absorbance of the Coomassie blue-stained proteins was measured at 550 nm.

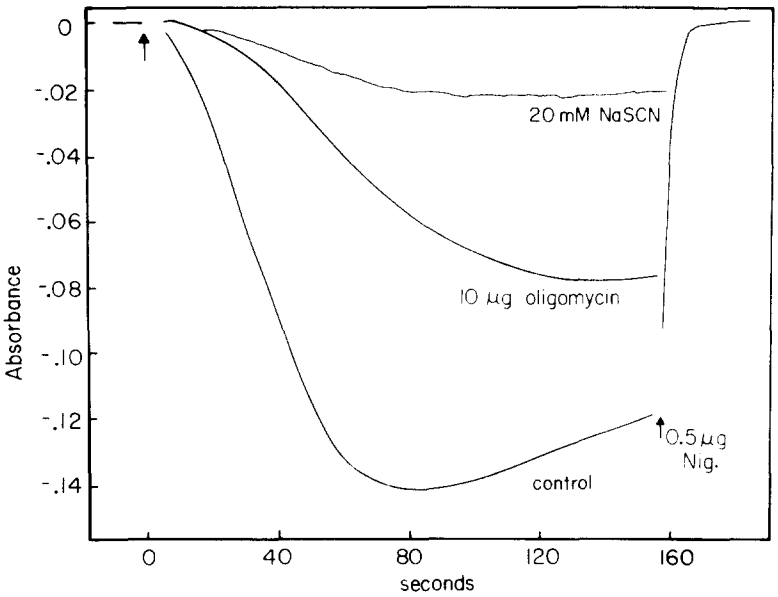

Fig. 5. Absorbance of acridine orange in energized FFI. Following the preloading procedure detailed in Materials and Methods, a 350 µl aliquot was transferred to a microcuvette to begin a 10 min incubation in either 20 mM NaSCN or 10 µg oligomycin. 5 µM acridine orange was added and at zero time, 0.8 mM MgATP, pH 7.4, addition produced the absorbance changes (sample 496 nm, reference 446 nm) monitored. The control signal was incubated similarly but in the absence of NaSCN or oligomycin.

energization in each microsomal equilibrium density fraction is presented in Fig. 6a. While there were preparational differences in the rate of development and magnitude of the acridine orange signal, the large response of this probe in each equilibrium density fraction was a consistent finding. This signal, qualitatively identical to signal development in the FFI fraction, was characterized by its dependence on prior KCl equilibration, its dissipation by nigericin or

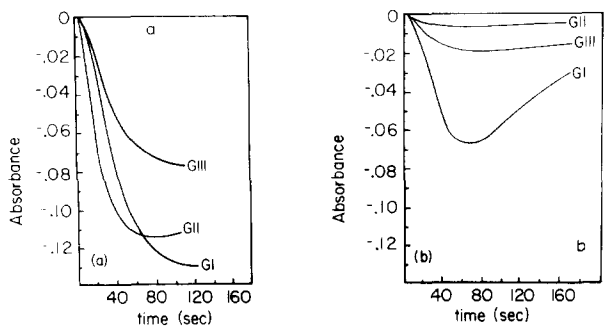

Fig. 6. Absorbance of acridine orange and DOCC (with TCS) in energized sucrose gradient fractions. Aliquots of each membrane fraction were prepared as detailed in Materials and Methods. (a) 5 µM acridine orange was added to each fraction. At zero time, 0.8 mM ATP, pH 7.4, addition produced the absorbance changes monitored at, sample 496 nm, reference 446 nm. (b) The procedure was identical as in (a) except that 4 µM DOCC and 6 µM TCS were substituted for acridine orange. DOCC absorbance was measured at sample 588 nm, reference 636 nm. GI, GII and GIII are the membrane fractions designated in the text.

tributyltin and its enhancement when valinomycin was added before ATP depletion.

Diethyloxadicarbocyanine. The DOCC + TCS measurement of the ability of each fraction to generate a potential upon ATP addition is recorded in part b of Fig. 6. In contrast to the activity observed with acridine orange in each fraction, the DOCC + TCS measured potential did show a gradient resolved enhancement. As shown in Fig. 6b, the largest DOCC + TCS absorbance changes were generated in the lightest fraction. The inverse relationship between DOCC + TCS signal development and the equilibrium density of the fractions was a consistent observation between preparations and could be accounted for by a progressive increase in other conductances with density. As noted for hog vesicles [24] this signal development was dependent upon the inclusion of TCS in the reaction media and prior equilibration with KCl. In the absence of 6 μM TCS, the ATP-dependent absorption changes of DOCC were of small magnitude and slow in development (results not shown). This signal was reversed by the addition of valinomycin or nigericin.

The TCS-dependent DOCC response was also present in the anodic free flow peak. In this fraction, the magnitude of the DOCC + TCS signal was small in comparison to the acridine orange response of the same material. Fig. 7 compares the ATP-dependent signal in the anodic peak after substitution of K_2SO_4 for KCl. In K_2SO_4 media the absorbance maximum increases 28% over that obtained in the KCl media, while the t_{max} of the signal was delayed from 80 s in KCl to 120 s in the K_2SO_4. In both cases the signal was nigericin sensitive.

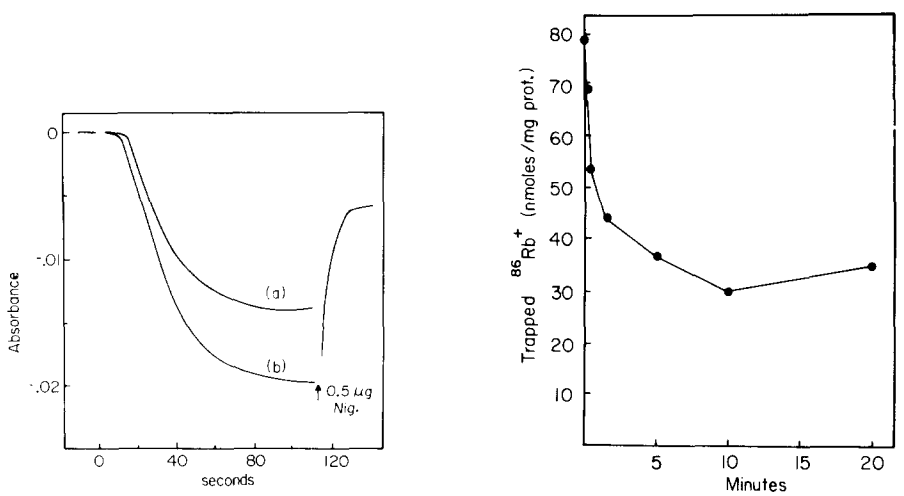

Fig. 7. Comparison of the DOCC (with TCS) absorbance signal in KCl and K_2SO_4 media. The FFI membrane fraction was incubated in either KCl or K_2SO_4 media as outlined in Materials and Methods. 350-μl aliquots were transferred to microcuvettes and 4 μM DOCC and 6 μM TCS added. At zero time, 0.8 mM MgATP (pH 7.4) was added and the absorbance monitored at sample 598 nm, reference 636 nm. Curve a, the absorbance signal of the FFI material incubated in KCl media; curve b, material incubated in K_2SO_4 media.

Fig. 8. 2 mM MgATP (pH 6.1) was added at zero time to the FFI membrane fraction previously incubated with $^{86}Rb^+$ as detailed in Materials and Methods. Each point, representing the amount of trapped $^{86}Rb^+$ remaining at that time, is the average of two experiments.

TABLE VI

NaSCN SENSITIVITY OF $^{86}Rb^+$ EFFLUX

FFI membranes	Trapped $^{86}Rb^+$ following ATP addition (nmol)		
	0	90 s	10 min
Control	105	80.7	56.5
+20 mM NaSCN	105	79.1	53.6

With a 10 min incubation, 20 mM SCN^- inhibited the DOCC + TCS signal by greater than 90%.

K^+ efflux. The identification of K^+ as a transported ion was observed as the ATP-dependent loss of trapped $^{86}Rb^+$ from vesicles previously incubated in $^{86}RbCl$. Preincubation of the material for 2 h at room temperature was used for equilibration of the isotope within the membrane-bound space. Calculation of the counts trapped by the FFI material at this time gave an apparent volume of 1.3 μl/mg. The addition of 2 mM Mg^{2+}-ATP caused a rapid loss of trapped $^{86}Rb^+$ which accounted for 62% of the initial equilibrated $^{86}Rb^+$. The kinetics of this $^{86}Rb^+$ disappearance from the anodic material are shown in Fig. 8. 71% of the total counts sensitive to ATP were lost within the first 90 s. A slow loss during the subsequent 8.5 min accounted for the remaining efflux. After 10 min (ATP depletion occurs about this time) there is a slow re-equilibration of the $^{86}Rb^+$). Similar data were obtained when $^{86}RbCl$ was used in the presence of KCl.

In another preparation, the normal ATP-dependent loss of trapped $^{86}Rb^+$ was compared to vesicles previously incubated with 20 mM NaSCN. Table VI indicates virtually no effect of the NaSCN on either the 90 s or 10 min values following ATP addition.

Discussion

Fractionation of frog gastric mucosal homogenates by differential and density gradient centrifugation has been described previously [8]. We were unable, by a variety of procedures to separate a K^+-activated ATPase from an ATPase which had mitochondrial ATPase characteristics, such as oligomycin sensitivity and inhibition by mitochondrial ATPase inhibitor protein [26,27]. However, using free flow electrophoresis, separation of two groups of particles was achieved. The anodic fraction was enriched in K^+-ATPase, whereas the cathodic fraction was enriched in HCO_3^--activated ATPase. The level of the two ATPases in the microsomal fraction was such that less than 5% (3.4%) could be accounted for as the K^+-activated component, whereas in the anodic fraction 32.0% was due to the K^+ component. This K^+-component insensitivity to 20 mM SCN^- and oligomycin was similar to hog enzyme [10]. Spectral analysis of the two fractions showed the continued presence of mitochondrial redox components, but significant depletion in the anodic fraction compared to the cathodic fraction. A more striking segregation of markers was found using polyacrylamide gel electrophoresis in SDS. The 100 000 dalton peptides, which characterizes the K^+-ATPase of dog [12,13], hog [15,16], rabbit [14] or man

[17] was found exclusively in the anodic fraction, whereas the cathodic fraction had a 44 000 dalton peptide as its major component. The expected subunit pattern of the mitochondrial F_1 ATPase, however, was not observed. In accordance with expectation, the phosphorylation of membrane peptide by [γ-^{32}P]ATP occurred in the anodic fraction. The level found, 266 pmol/mg ^{32}P is one fifth of that found in hog enzyme [31], but only 46% of the phosphorylation is discharged by K^+. Thus, the above data indicate, that in contrast to centrifugation methods, in our hands, free flow electrophoresis is capable of partially resolving ATPase activities of frog microsomes.

Both particulate fractions isolated by free electrophoresis are vesicular, in that, based on $^{86}Rb^+$ uptake, an equilibrium volume of 1.3 μl/mg is found. As for hog, Rb^+ loss dependent on the presence of ATP occurs only in the anodic fraction [11]. This loss occurs in two phases, a rapid phase accounting for 71% of total loss occurring within 90 s, and a slower phase lasting until the depletion of ATP. The efflux was insensitive to SCN^- and thus these data corresponded in large measure to those already described for hog [10,11]. Accordingly, frog gastric vesicles are capable of generating K^+ gradients in the presence of ATP.

There are several means of measuring proton gradients in vesicles such as electrometric techniques, potential dye probes, binding dyes such as acridine orange and weak bases such as 9-aminoacridine. Except for the potential dye probes, these techniques do not in general discriminate between plasma membrane or everted mitochondrial vesicles since both types could be expected to generate a ΔpH with the addition of ATP. However, in the case of the mitochondrial ATPase the pump mechanism is electrogenic and gradient or potential development is independent of added K^+ [28] whereas the hog gastric plasma membrane ATPase transport is neutral and K^+ dependent [10].

In the gradient fractions, acridine orange responses are found in all the fractions. Everted mitochondrial vesicles also show increased acridine orange binding with ATP addition [29], but since in the gastric vesicular experiments, K^+ was an absolute requirement and results from potential-sensitive dyes were negative, there is a question as to whether the mitochondrial contamination of the denser peaks was responsible for the dye signal.

With free flow fractionation, the only transport responses were observed in the K^+-ATPase enriched, HCO_3^--ATPase depleted fractions. It is possible that electrophoresis separates normally fused membranes, but it is more likely that this method simply enriches plasma membrane as distinct from other vesicular membrane structures. In the anodic fraction, therefore, it is possible to compare transport by frog membranes to those of hog.

The vesicular volume/mg protein of the frog preparation is about half of that of the hog. Using FFI membrane material and the pH electrode the change in external pH corresponds to an uptake, in equilibrated vesicles, of 19 nmol/μl, considerably less (1/5) than an average hog preparation. However, the Rb^+ efflux is close to that of the hog in terms of nmol/μl transported.

The presence of an HCl leak path and the absence of a large Rb^+ leak could account for the discrepancy, the H^+ being exchanged for Rb^+ by the pump and HCl leaking by an unspecified pathway. A back leak of OH^- in exchange for Cl^- would also result in this discrepancy.

The signal generated by the addition of ATP in the presence of acridine orange was similar in magnitude compared to that found in hog [24] in spite of the lower proton uptake values. The acridine orange signal is due to binding of the dye to negative sites induced by a pH gradient. The number of those sites could be a function of the phospholipid composition of the membrane (e.g. the per cent and orientation of phosphatidylserine residues) and hence quantitative correlation may not be anticipated betweeen species. The time of formation of the maximum dye signal was considerably delayed compared to the hog, but correlated with the fast Rb^+ efflux phase. This, coupled with the Rb^+ efflux found, would lead to the conclusion, as for the hog, that a K^+ for H^+ exchange is the transport mechanism.

An unequal stoichiometry, in the absence of shunting conductances would result in development of a potential difference. Positively or negatively charged dyes, such as DOCC or $diBAC_4(5)$ (oxonol) would then show a response to ATP addition. This was not the case, but as for the hog, the addition of a protonophore to the DOCC experiment, resulted in the development of a potential difference, interior negative, explained as due to H^+ diffusion potential across the protonophonic conductance [24]. This indicates the development of a H^+ gradient, and also the absence of a large enough shunting conductance to short circuit the H^+ diffusion potential.

The in vitro frog mucosa, in the absence of Cl^-, but in the presence of SO_4^{2-}, shows an inverted potential difference interpreted as due to the electrogenic H^+ pump [1]. In hog vesicles, replacement of Cl^- by SO_4^{2-} reduced the rate of development and magnitude of all the transport signals [10], unless the vesicles had been aged or treated with trypsin or chymotrypsin [30]. In this case, partial restoration of the signals could be achieved by Cl^- removal and SO_4^{2-} substitution. In the case of frog free flow fraction I, the signal generated by DOCC in the presence of TCS was increased by the SO_4^{2-} substitution. This is explained as being due to removal of a Cl^- conductance which, in the presence of a TCS-induced H^+ conductance, partially shunts the H^+ diffusion potential. Thus, frog vesicles may contain a significant Cl^- conductance perhaps contributing to the discrepancy between H^+ and Rb^+ fluxes, as noted above. The absence of Cl^- however, did not result in a response of the negatively charged $diBAC_4(5)$ which would have occurred had an electrogenic pump been unmasked.

Another difference between hog and frog, qualitative rather than quantitative, was the abolition of the acridine orange and DOCC + TCS response by 20 mM SCN^-. Since the K^+-ATPase hydrolytic activity was insensitive to this ion it seems reasonable that the action of SCN^- influences the coupling of ATP turnover to H^+ or Rb^+ transport. As Rb^+ transport was unaffected, SCN^- apparently uncouples H^+ from Rb^+ transport in frog vesicles. The simplest interpretation is that SCN^- provides an anion conductance path allowing H^+ to leak across the whole membrane, or uncouples an intramembranal transport compartment of bound H^+. Since SCN^- addition after the signal had developed was less effective than a 10 min incubation with SCN^- before ATP addition, we favor an uncoupling action at an intramembranal site, rather than induction of a transmembranal leak. Indeed the latter would require an associated large H^+ conductance, and although the H^+ conductance exceeds the K^+ conductance, it

is still too small to be detected by DOCC alone. A series pump model, using components (e.g. $\alpha_2\,\beta_2$) of the mitochondrial F_1 ATPase and the specific gastric $H^+ + K^+$)-ATPase would show many of the above properties.

Thus, frog mucosa, as for hog, contains a membrane which is capable of H^+ and K^+ transport, as well as having an associated K^+-ATPase activity and a phosphorylatable M_r 100 000 peptide. Differences between hog and frog membrane properties are both quantitative and qualitative, but the general aspects of the transport phenomena are similar.

Acknowledgement

This work was supported in part by grants NIH AM15878 and AM21588 and NSF PCM 77-18951.

References

1 Rehm, W.S. (1972) Metabolic Transport (Hokin, L.E., ed.), pp. 187–241, Academic Press
2 Sachs, G., Spenney, J.R. and Lewin, M. (1978) Physiol. Rev. 58, 106–173
3 Forte, J.G. and Solberg, L.A. (1973) International Encyclopedia of Pharmacology and Therapeutics (Holton, P., ed.), pp. 195–260, Permagon Press
4 Hersey, S.J. (1974) Biochim. Biophys. Acta 344, 157–203
5 Rehm, W.S. (1965) Fed. Proc. 24, 1387–1395
6 Rabon, E.C., Sarau, H.M., Rehm, W.S. and Sachs, G. (1977) J. Membrane Biol. 35, 189–204
7 Durbin, R.P., Michelangeli, F. and Michel, A. (1974) Biochim. Biophys. Acta 367, 177–189
8 Ganser, A.L. and Forte, J.G. (1973) (Biochim. Biophys. Acta 307, 169–180
9 Sarau, H.M., Foley, J., Moonsamy, G., Wiebelhaus, V.D. and Sachs, G. (1975) J. Biol. Chem. 250, 8321–8329
10 Sachs, G., Chang, H.H., Rabon, E., Schakmann, R., Lewin, M. and Saccomani, G. (1976) J. Biol. Chem. 251, 7690–7698
11 Schackmann, R., Schwartz, A., Saccomani, G. and Sachs, G. (1977) J. Membrane Biol. 32, 361–381
12 Lee, J.E., Simpson, •,• and Scholes, P. (1974) Biochem. Biophys. Res. Commun. 60, 825–834
13 Saccomani, G., Shah, G., Spenney, J.G. and Sachs, G. (1975) J. Biol. Chem. 250, 4802–4809
14 Forte, J.G., Ganser, A.L. and Tanisawa, A.S. (1974) Ann. N.Y. Acad. Sci. 242, 255–267
15 Forte, J.G., Ganser, A., Beesly, R. and Forte, T.M. (1975) Gastroenterology 69, 175–189
16 Saccomani, G., Stewart, H.B., Shaw, D., Lewin, M. and Sachs, G. (1977) Biochim. Biophys. Acta 465, 311–330
17 Saccomani, G., Chang, H.H., Crago, S., Mihas, A.A. and Sachs, G. (1978) J. Clin. Invest., in press
18 Forte, J.G., Ray, T.K. and Poulter, J.L. (1972) J. Appl. Physiol. 32, 714–717
19 Hannig, K., Glick, D. and Rosenbaum, R.M. (1972) Techniques of Biochemical and Biophysical Morphology, p. 191, J. Wiley and Sons
20 Lowry, O.H., Rosebrough, N.J., Farr, A.L. and Randall, R.J. (1951) J. Biol. Chem. 193, 265–275
21 Yoda, A., and Hokin, L.E. (1970) Biochem. Biophys. Res. Commun. 40, 880–884
22 Fiske, C.H. Subbarow, Y. (1925) J. Biol. Chem. 66, 375–400
23 Chance, B. and Williams, G.A. (1955) J. Biol. Chem. 217, 395–407
24 Rabon, E., Chang, H.H. and Sachs, G. (1978) Biochemistry 17, 3345–3353
25 Avruch, J. and Fairbanks, G. (1972) Proc. Natl. Acad. Sci. U.S. 69, 1216–1220
26 Hortsman, L.L. and Racker, E. (1970) J. Biol. Chem. 245, 1336–1344
27 Kagawa, Y. and Racker, E. (1966) J. Biol. Chem. 241, 2461–2466
28 Azzone, G.F. and Massari, S. (1973) Biochim. Biophys. Acta 301, 195–226
29 Dell'Antone, P., Colonna, R. and Azzone, G.F. (1971) Biochim. Biophys. Acta 234, 541–544
30 Rabon, E., Kajdos, I. and Sachs, G. (1978) Biochim. Biophys. Acta submitted
31 Sach, G., Rabon, E. and Saccomani, G. (1978) International Symposium on Bioenergetics, Kobe, Japan, Academic Press, in press